# Electronic Supplementary Information

# 1. Instrumentation:

**Thermogravimetric analysis** (TGA) was performed on METTLER TOLEDO TGA 2 STARe system under air flow with a flow rate of 60 mL $min^{-1}$. A polycrystalline aluminum oxide crucible (PCA) was used. Samples were analyzed in a temperature range of 303.15−823.15 K. A heating rate of 10 K $min^{-1}$ was applied.

**Attenuated total reflectance-Fourier-transformed infrared spectroscopy** (ATR-FT-IR) was performed using a Bruker Alpha II equipped with an ATR Platinum Diamond unit. The data were recorded with 24 scans at a resolution of 4 $cm^{-1}$. All spectra were background-corrected within the Bruker OPUS 8.1 program suite.

**UV/Vis/NIR spectroscopy** was performed on a Cary 3500 UV/Vis/NIR spectrophotometer equipped with a Xenon flash lamp (250 Hz). Measurements were performed in screw cap quartz glass cuvettes (d = 10.0 mm) with rubber septa.

**Gas chromatography** was performed on a Shimadzu Nexis GC-2030 equipped with a dielectric-barrier discharge ionization detector and a split injection unit with a split ratio of 1:20. Helium was chosen as the carrier gas. The column was heated to a constant temperature of 80˚C.

**Chemicals:** All chemical reagents were obtained commercially and used as received unless stated otherwise. $(NH_4)_2[Mo_3S_{13}]\cdot 2H_2O$ was prepared according to the literature.[1]

**Vials:** All vials were purchased from Biotage with crimp caps made of aluminum with silicone rubber/Teflon septa. Outer diameter: 17 mm, inner diameter: 15 mm, length: 85 mm total volume: ~11.0 mL (https://selekt.biotage.com/hubfs/PPS449.v1%20-%20Microwave%20Reaction%20Vials.pdf c) )

# 2. Experimental data

## 2.1. Synthesis of $(NH_4)_2[Mo_3S_{13}]\cdot 2H_2O$

Synthesis was performed by Moritz Jahn and Laura Haxha.

The thiomolybdate $(NH_4)_2[Mo_3S_{13}]\cdot 2H_2O$ was synthesized using a modified method based on the work of MÜLLER et al.[1] $(NH_4)_6[Mo_7O_{24}]\cdot 4\ H_2O$ (4.0 g, 3.2 mmol) was dissolved in 20 mL of water in a round-bottom flask. An ammonium polysulfide ($(NH_4)_2S_x$) solution (120 mL, 25 wt.-%) was added, and the flask was covered with a watch glass. The solution was heated to 96 °C for five days without stirring. Dark-red crystals of $(NH_4)_2[Mo_3S_{13}]\cdot 2H_2O$ formed, which were collected by filtration, then washed with water, ethanol, carbon disulfide and ether. The final product was air-dried.

**Yield:** 5.5 g (7.04 mmol; 91.4 % based on Mo)
**UV-VIS bands (nm):** $\lambda_{max}$ = 451
**ATR-FTIR bands ($cm^{-1}$):** 1478 (s), 537 (s) ,511 (s)
**TGA:** **(1)** Temp: 30 °C – 295 °C, calculated mass loss: 6.2 %, possible loss: 2 $H_2O$
**(2)** Temp: 295 °C – 550 °C, calculated mass loss: 31.5 %, possible loss: 2 $NH_3$, 6 S

## 2.2. Experimental Plan

The following experiment plan was created by Minitab for a full factorial screening approach with three factors. Since only the same frequency and duty cycle but all LED currents could be measured on the same day, blocks were created manually. Every factor setting combination was measured on three individual days (triplicate) and on each day three samples were prepared.

Table S1: Experiment plan created by Minitab and adapted to use.

| Measurement day | Frequency (Hz) | LED current (mA) | Duty cycle (%) |
|---|---|---|---|
| 1 | 2 | 350, 500, 700 | 25 |
| 2 | 50 | 350, 500, 700 | 75 |
| 3 | 2 | 350, 500, 700 | 75 |
| 4 | 50 | 350, 500, 700 | 25 |
| 5 | 2 | 350, 500, 700 | 75 |
| 6 | 50 | 350, 500, 700 | 75 |
| 7 | 2 | 350, 500, 700 | 75 |
| 8 | 2 | 350, 500, 700 | 25 |
| 9 | 50 | 350, 500, 700 | 25 |
| 10 | 50 | 350, 500, 700 | 25 |
| 11 | 2 | 350, 500, 700 | 25 |
| 12 | 50 | 350, 500, 700 | 75 |

## 2.3. Sample preparation

**GC measurements:** Stock solutions for the catalyst $(NH_4)_2[Mo_3S_{13}]$ ($c = 3 \cdot 10^{-4}$ M), the photosensitizer ($c = 1 \cdot 10^{-5}$ M) and the sacrificial electron donor (sodium ascorbate and ascorbic acid, molar ratio: 4:5 ; $c = 1 \cdot 10^{-1}$ M in water) were prepared for the catalytic systems. The catalyst solution was prepared by dissolving $(NH_4)_2[Mo_3S_{13}]$ in degassed methanol and was afterwards stored under $N_2$ atmosphere. The photo sensitizer $[Ru(bpy)_3](PF_6)_2$ was dissolved in methanol. For the SED solution, sodium ascorbate and ascorbic acid were dissolved in water. The stock solutions were stored while keeping them protected from light.

Before mixing the individual components, the catalyst solution was diluted with methanol by a factor of 100, resulting in a concentration of $c = 1 \cdot 10^{-6}$ M. The stock solutions for the PS and the SED, the solvent as well as the diluted catalyst solution were combined in crimp vials with a total volume of 4 mL per vial. The vials were sealed with crimper lids equipped with silicone septa and purged with nitrogen for one hour. Additionally, the septa were covered with clear nail polish after being pierced by the syringes to prevent leakage. Before measurements, the nail polish was removed to allow sampling of the gas headspace.

**UV/Vis measurements**: For determination of the quantum yield of the photosensitizer, stock solutions were prepared analogously to the GC measurements sample preparation. The cuvettes were sealed with silicon septa equipped screw caps and then purged for 10 min with nitrogen before measurements were performed.

For determination of the photodegradation of the **{$Mo_3$}** cluster, the solid was weighed into screw cap vials and then dissolved in a degassed MeOH:$H_2O$ (9:1, v:v) mixture. The solution was then put in an ultrasonic bath for 15 min and transferred in the cuvettes. The cuvettes were sealed with silicone septa equipped screw caps and purged with nitrogen for 10 min.

## 2.4. Procedure of GC measurements

After successful preparation, the samples were placed in the photoreactor. The photoreactor was equipped with a hexagonal holding unit with six individual spots for the crimp vials. For every hydrogen measurement, at least three individual samples were prepared. Before the hydrogen measurement started, the GC was checked with three air measurements to obtain a reproducible baseline. The samples were measured at the beginning of the irradiation, and at the respective time intervals of irradiation.

## 2.5. Photoreactor setup

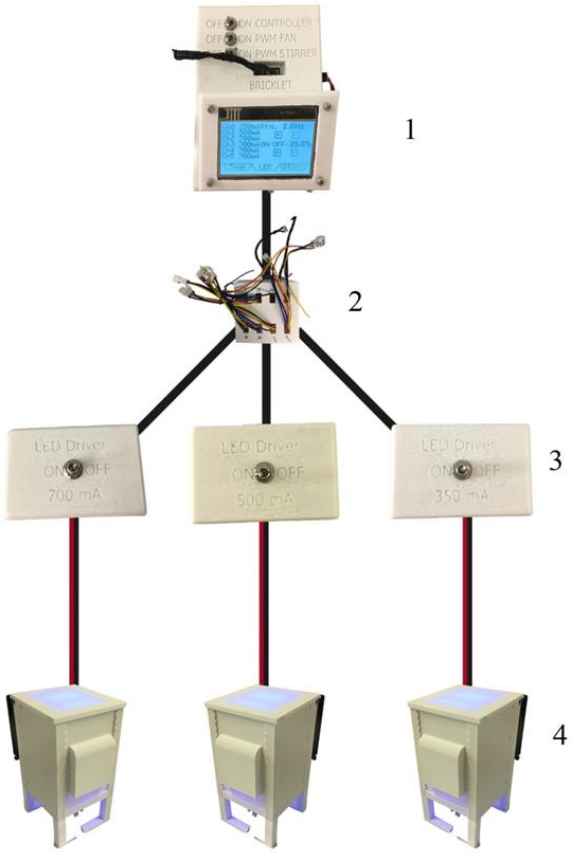


Figure S1: Photograph of the photoreactor setup, with a controller module (1), an In/Out-Bricklet (2), three LED drivers (3) and three photoreactors (4).

The controller module enables the control of the duty cycle and the frequency. The In/Out bricklet forwards the signal to the individual LED-Drivers which determine the LED current and therefore indirectly the light power. The LED is positioned at the bottom of the photoreactor. The whole design was created by Kowalzcyk et al.[2]
The 90x90x140 mm modular photoreactor was chosen for these experiments and printed with white PLA. The vial holder was placed in the 10$^{th}$ vertical holder slot above the LED and the lower distance between the bottom of the reactor and the vials bottom was 22 mm. The radius of the holder was 43 mm.

An instruction manual and CAD files to print the reactor and controller units as well as the python script that was used in the controller unit to set frequency and duty cycle can be found here:

https://github.com/photonZfeed/modularPhotoreactor

Information about the used LED:
https://look.ams-osram.com/m/6208f3ef096a8da0/original/LZ1-10B202.pdf
https://look.ams-osram.com/m/77b624bf9a989535/original/LZ1-00B202.pdf

LED Driver:
https://www.meanwellusa.com/webapp/product/search.aspx?prod=LDD-L OSRAM
LED Engin LZ1-00B202:
https://www.mouser.de/datasheet/3/5912/1/LZ1_00B202_EN.pdf

The sample positions of the vials were chosen randomly to eliminate the systematic error of heterogeneous irradiation conditions in a photoreactor.

## 2.6. LED Power Determination

To measure the power of the LED a PM400 Optical Power Meter by Thorlabs was used. Power was measured at five or six positions of the photoreactor for different currents in duplicate or triplicate. The chosen positions were in radial order and at a height comparable to bottom of the sample flasks.

Table S2: Measured LED power P for different positions 1-6 in the photoreactor with individual measurement error. Red fields represent outliers which were rejected when calculating averages and standard deviations.

| $I_{LED}$ | P1 (mW) | P2 (mW) | P3 (mW) | P4 (mW) | P5 (mW) | P6 (mW) |
|---|---|---|---|---|---|---|
| 350 mA (1) | 7.6 ± 0.3 | 7.0± 0.3 | 6.5 ± 0.3 | 5.3 ± 0.3 | 7.0 ± 0.2 | 7.4 ± 0.3 |
| 350 mA (2) | 7.4 ± 0.2 | 7.4 ± 0.3 | 6.8 ± 0.3 | 6.0 ± 0.3 | 7.2 ± 0.3 | 7.3 ± 0.3 |
| 350 mA (3) | 7.5 ± 0.3 | 6.9 ± 0.2 | 6.2 ± 0.3 | 5.6 ± 0.3 | 7.4 ± 0.3 | 7.7 ± 0.3 |
| 500 mA (1) | 9.6 ± 0.2 | 10.7 ± 0.3 | 10.6 ± 0.4 | 7.6 ± 0.3 | 6.4 ± 0.3 | -- |
| 500 mA (2) | 9.3 ± 0.3 | 10.8 ± 0.3 | 10.8 ± 0.3 | 8.4 ± 0.3 | 7.0 ± 0.3 | -- |
| 700 mA (1) | 14.4 ± 0.4 | 13.5 ± 0.3 | 14.1 ± 0.3 | 11.6 ± 0.4 | 13.1 ± 0.3 | -- |
| 700 mA (2) | 13.2 ± 0.3 | 13.7 ± 0.2 | 12.2 ± 0.3 | 12.0 ± 0.3 | 12.4 ± 0.3 | -- |

Table S3: Average LED power for different current supplies and the corresponding photon fluence rates q (calculated using equation 6). All values are only given for the area of 1 $cm^2$ of the detector.

| $I_{LED}$ (mA) | $P_{LED}$ (mW) | $\Delta P_{LED}$ (mW) | q (nmol $s^{-1}$ $cm^{-2}$) | Δq (nmol $s^{-1}$ $cm^{-2}$) |
|---|---|---|---|---|
| 350 | 6.9 | ± 1.0 | 27 | ± 4 |
| 500 | 9.4 | ± 1.0 | 37 | ± 4 |
| 700 | 13.0 | ± 1.0 | 51 | ± 4 |

## 2.7. FT-IR Spectrum of $(NH_4)_2[Mo_3S_{13}]$

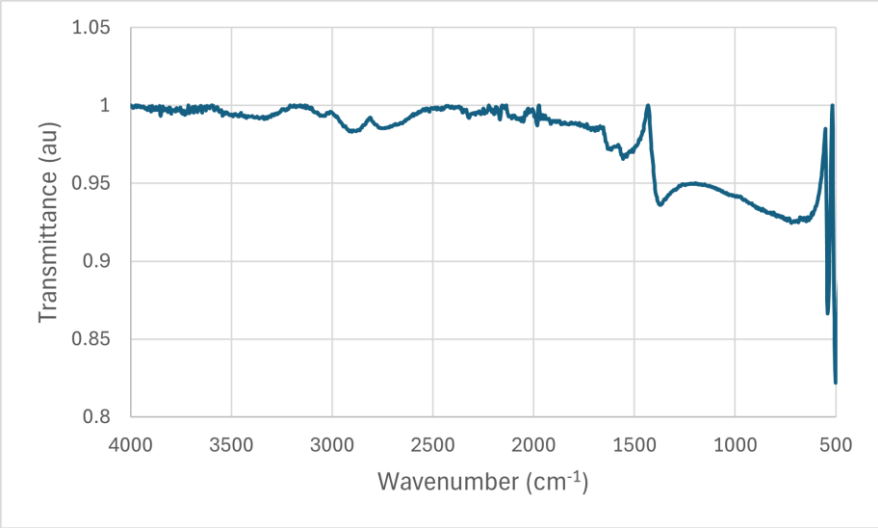


Figure S2: FT-IR spectrum of $(NH_4)_2[Mo_3S_{13}]\cdot 2H_2O$.

## 2.8. TGA Analysis

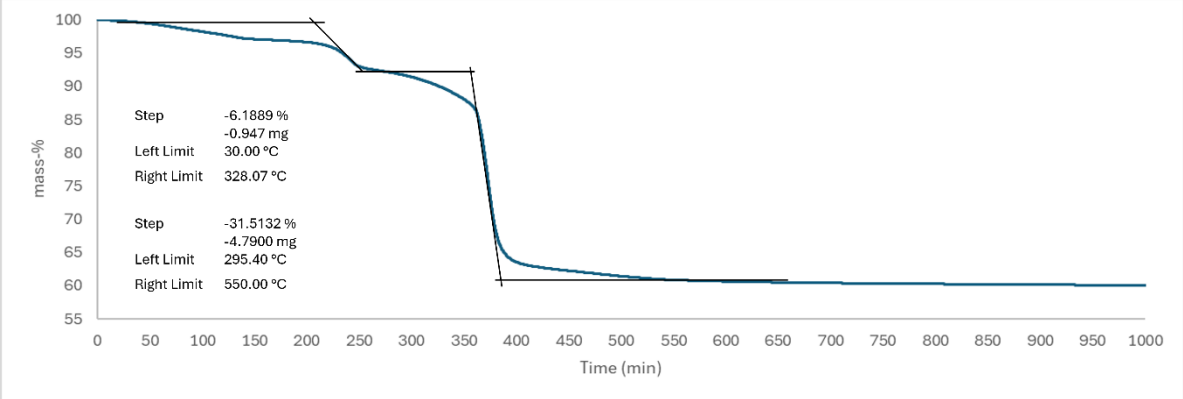


Figure S3: TGA of $(NH_4)_2[Mo_3S_{13}]\cdot 2H_2O$.

## 2.9. Calculation of TON

To determine the TON, the volume of the gas phase in the vial was calculated using the following equation:

$$V_{gas} = V_{vial} - V_{sol} \quad [1]$$

$V_{gas}$: gas volume of the vial. $V_{vial}$: total volume of the vial. $V_{sol}$: volume of the catalytic solution. The sample volume taken is 100 µL. To calculate the absolute amount of hydrogen evolved a vial specific factor $k_{vial}$ must be calculated using equation 2:

$$k_{vial} = \frac{V_{gas}}{100\ \mu L} \quad [2]$$

The absolute amount of hydrogen evolved $n_{H2,abs}$ can then be determined with the with the measured amount of hydrogen $n_{measured}$ per 100 µL, using the following equation:

$$n_{H_2,abs} = n_{measured} \cdot k_{vial} \quad [3]$$

The TON is the ratio of the absolute amount of hydrogen $n_{H2,abs}$ and the amount of catalyst in the solution $n_{cat}$:

$$TON = \frac{n_{H_2,abs}}{n_{cat}} \quad [4]$$

Table S4: Measured TON for experimental plan and DoE. Red fields represent outlier measurements with high errors that were not used when calculating averages and standard deviations.

| **50 Hz, 25 %** | | | **50 Hz, 75 %** | | | **2 Hz, 25 %** | | | **2 Hz, 75 %** | | |
|---|---|---|---|---|---|---|---|---|---|---|---|
| **TON 350 mA** | **TON 500 mA** | **TON 700 mA** | **TON 350 mA** | **TON 500 mA** | **TON 700 mA** | **TON 350 mA** | **TON 500 mA** | **TON 700 mA** | **TON 350 mA** | **TON 500 mA** | **TON 700 mA** |
| 92 | 693 | 773 | 495 | 999 | 1360 | 491 | 267 | 480 | 950 | 980 | 1310 |
| 430 | 642 | 810 | 717 | 1110 | 1220 | 270 | 658 | 738 | 651 | 1110 | 1040 |
| 12 | 599 | 579 | 849 | 1170 | 1560 | 528 | 708 | 477 | 867 | 906 | 1420 |
| 361 | 394 | 429 | 62 | 623 | 603 | 207 | 482 | 666 | 314 | 755 | 1330 |
| 68 | 305 | 344 | 430 | 473 | 724 | 286 | 282 | 570 | 545 | 1220 | 999 |
| 99 | 321 | 415 | 363 | 568 | 600 | 338 | 521 | 14 | 430 | 1110 | 1130 |
| 140 | 61 | 812 | 359 | 144 | * | 195 | 309 | 418 | 380 | 607 | 850 |
| 361 | 600 | 779 | 329 | 232 | 547 | 263 | 223 | 517 | 300 | 766 | 838 |
| 300 | 586 | 653 | 236 | 390 | 867 | 194 | 346 | 446 | 765 | 873 | 1190 |

Table S5: TON for 350 mA static irradiation.

| **Number** | **TON** | **Number** | **TON** |
|---|---|---|---|
| 1 | 447 | 12 | 437 |
| 2 | 245 | 13 | 498 |
| 3 | 219 | 14 | 678 |
| 4 | 219 | 15 | 501 |
| 5 | 396 | 16 | 826 |
| 6 | 123 | 17 | 415 |
| 7 | 70 | 18 | 233 |
| 8 | 104 | 19 | 277 |
| 9 | 116 | 20 | 210 |
| 10 | 115 | 21 | 101 |
| 11 | 509 | 22 | 359 |

Table S6: TON for optimized irradiation settings:700 mA, 2 Hz, 75 %.

| Number | TON |
|---|---|
| 1 | 1520 |
| 2 | 1430 |
| 3 | 1600 |
| 4 | 1190 |
| 5 | 1370 |
| 6 | 1290 |
| 7 | 1600 |
| 8 | 1350 |
| 9 | 1230 |
| 10 | 1210 |
| 11 | 1110 |

Table S7: TON at 700 mA static irradiation.

| Vial number | TON |
|---|---|
| 1 | 430 |
| 2 | 988 |
| 3 | 831 |
| 4 | 601 |
| 5 | 500 |
| 6 | 665 |

## 2.10. Time dependent TON

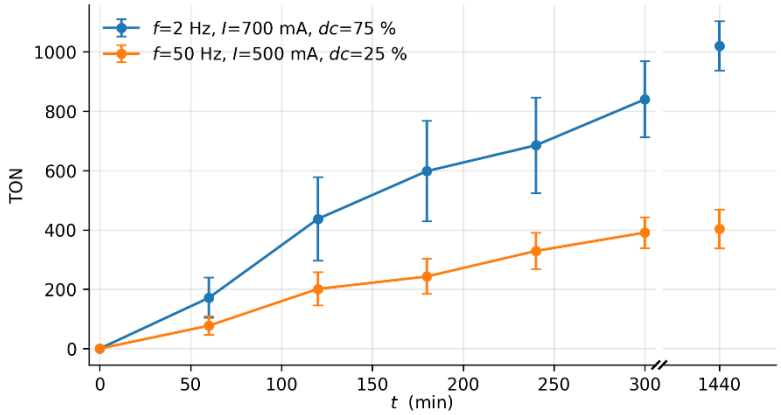


Figure S4: Time dependent TON for optimized irradiation conditions.

Since the system is close to an end after 5 hours, the overall performance is represented at the measurements taken once after 5 h of irradiation.

## 2.11. Calculation of photonic efficiency (PE)

The photonic efficiency PE is determined using the photon fluence rate *q* which is calculated based on the experimentally determined power *P* of the LED, the emission wavelength λ, the Planck constant *h*, the speed of light *c* and the Avogadro constant $N_A$.[3]

$$q = \frac{P \cdot \lambda}{h \cdot c \cdot N_A} \quad [6]$$

The total number of photons $n_{ph}$ can be calculated by multiplying the photon fluence rate *q* with the time *t*, the duty cycle (0.25 or 0.75) and the area $A_{Vial}$ of the vial (= 1.227 cm$^2$).

$$n_{ph} = q \cdot t \cdot \mathrm{dc} \cdot A_{Vial} \quad [7]$$

The PE is calculated using equation [8].

$$\mathrm{PE} = \frac{n_{H_2,abs}}{n_{ph}} \quad [8]$$

Table S8: PE calculated based on averaged TONs. The last two rows represent static irradiation.

| **LED current (mA)** | **Frequency (Hz)** | **Duty cycle (%)** | **PE (·10$^{-3}$)** |
|---|---|---|---|
| 350 | 50 | 25 | 1.7 ± 1.4 |
| 500 | | | 3.0 ± 1.1 |
| 700 | | | 2.6 ± 0.8 |
| 350 | 50 | 75 | 0.9 ± 0.5 |
| 500 | | | 0.9 ± 0.4 |
| 700 | | | 0.9 ± 0.3 |
| 350 | 2 | 25 | 2.5 ± 1.4 |
| 500 | | | 2.5 ± 1.1 |
| 700 | | | 2.3 ± 0.8 |
| 350 | 2 | 75 | 1.7 ± 0.6 |
| 500 | | | 1.8 ± 0.4 |
| 700 | | | 1.9 ± 0.3 |
| 350 | 0 (static conditions) | 100 (static conditions) | 0.7 ± 0.4 |
| 700 | 0 (static conditions) | 100 (static conditions) | 0.7 ± 0.2 |

## 2.12. UV/Vis Spectroscopy

All cuvettes were placed in holders so that the bottom of the cuvettes was 22 mm above the LED.

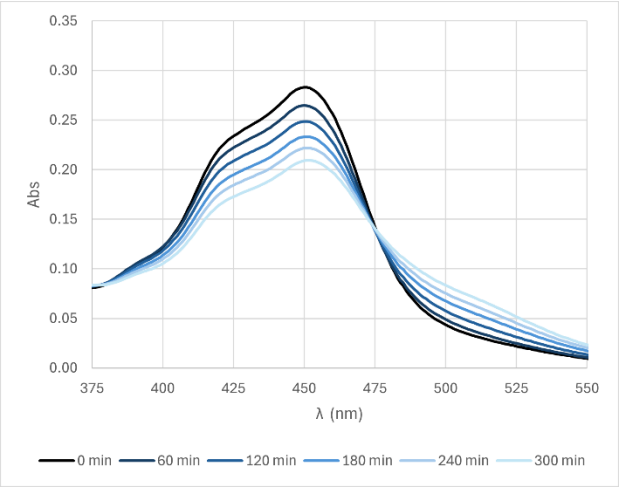


Figure S5: UV/Vis spectra over time for Ru (c = 20 µM in MeOH) irradiated under 700 mA static conditions.

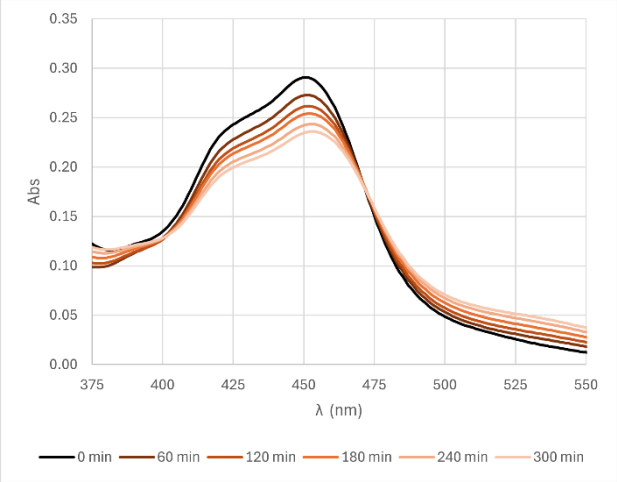


Figure S6: UV/Vis spectra over time for RuSEDCat ($c_{Ru}$= 20 µM, $c_{Mo3}$= 0.3 µM, $c_{SED}$= 100 µM in MeOH:$H_2O$; 9:1; v:v) irradiated under 700 mA static conditions.

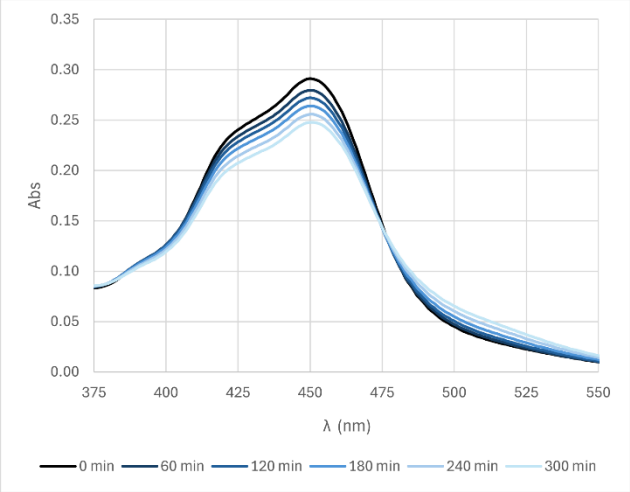


Figure S7: UV/Vis spectra over time for Ru (c = 20 µM in MeOH) irradiated under 500 mA static conditions.

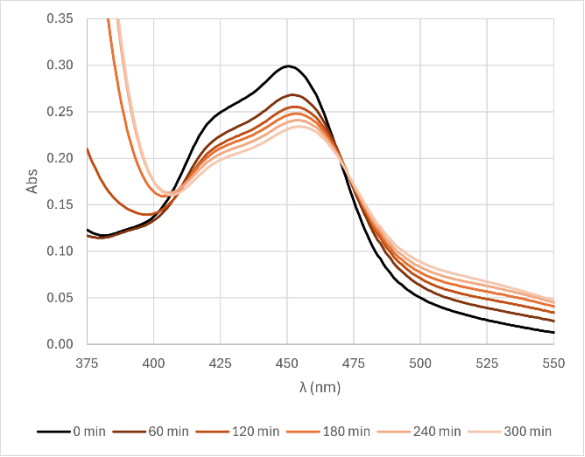


Figure S8: UV/Vis spectra over time for RuSEDCat ($c_{Ru}$= 20 µM, $c_{Mo3}$= 0.3 µM, $c_{SED}$= 100 µM in MeOH:$H_2O$; 9:1; v:v) irradiated under 500 mA static conditions.

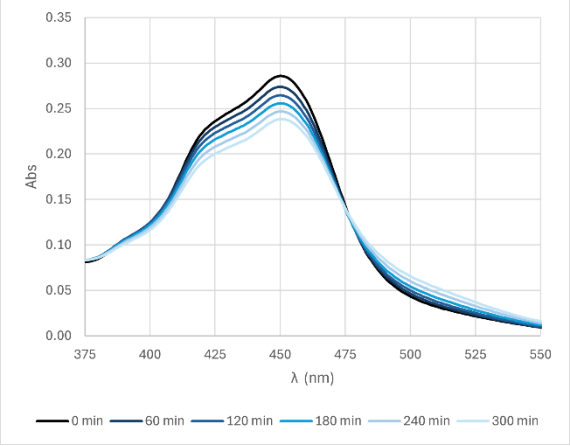


Figure S9: UV/Vis spectra over time for Ru (c = 20 µM in MeOH) irradiated under 700 mA, 2 Hz, 75% conditions.

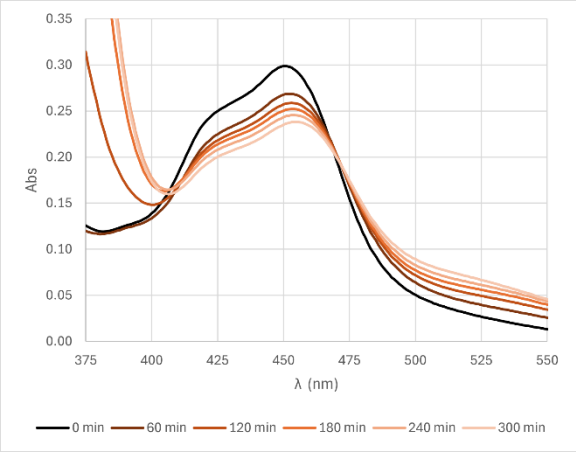


Figure S10: UV/Vis spectra over time for RuSEDCat ($c_{Ru}$= 20 µM, $c_{Mo3}$= 0.3 µM, $c_{SED}$= 100 µM in MeOH:$H_2O$; 9:1; v:v) irradiated under 700 mA, 2 Hz, 75 % conditions.

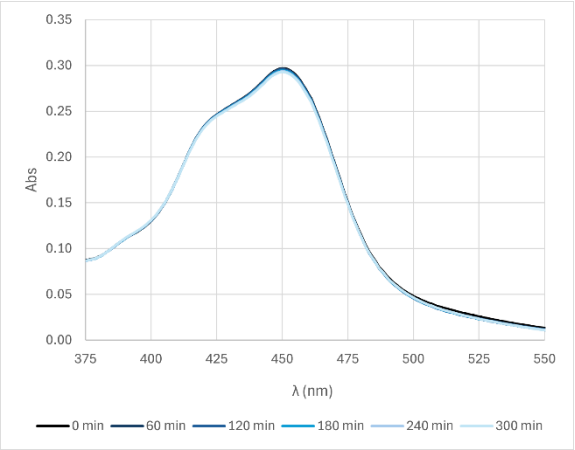


Figure S11: UV/Vis spectra over time for Ru (c = 20 µM in MeOH) irradiated under 500 mA, 50 Hz, 25% conditions.

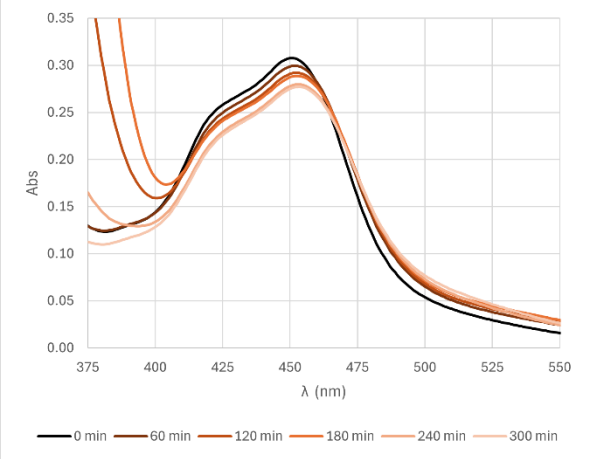


Figure S12: UV/Vis spectra over time for RuSEDCat ($c_{Ru}$= 20 µM, $c_{Mo3}$= 0.3 µM, $c_{SED}$= 100 µM in MeOH:$H_2O$; 9:1; v:v) irradiated under 500 mA, 50 Hz, 25 % conditions.

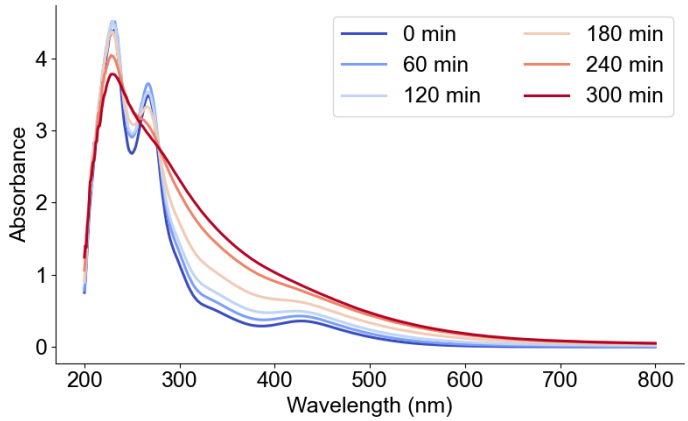


Figure S13: UV/Vis spectra over time for **{$Mo_3$}** (c = 0.1 mM) in MeOH:$H_2O$ (9:1, v:v) irradiated under 700 mA, 2 Hz, 75 % conditions.

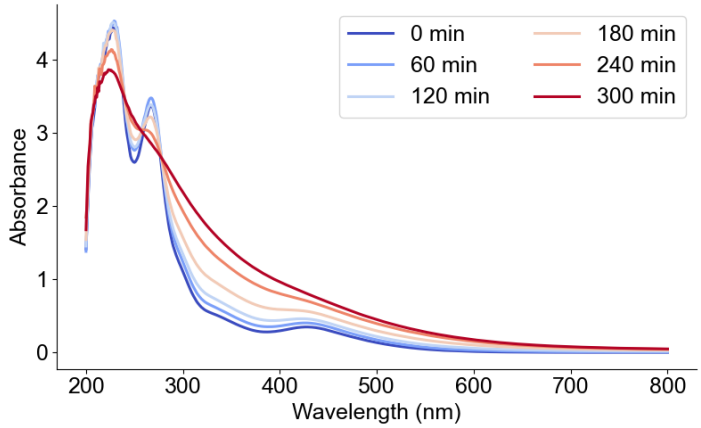


Figure S14: UV/Vis spectra over time for **{$Mo_3$}** (c = 0.1 mM) in MeOH:$H_2O$ (9:1, v:v) irradiated under 700 mA, 2 Hz, 75 % conditions.

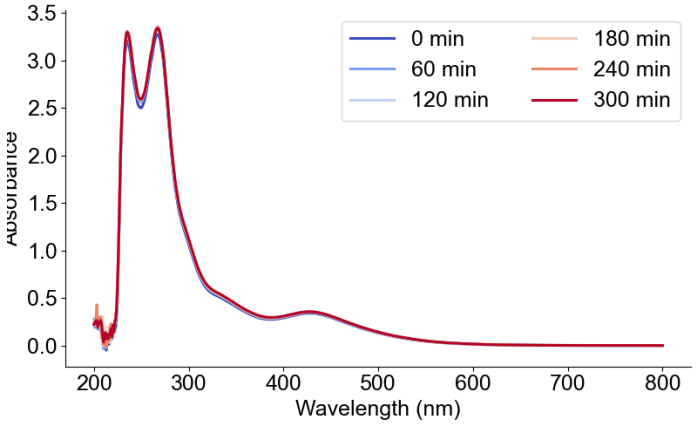


Figure S15:UV/Vis spectra over time for **{$Mo_3$}** (c = 0.1 mM) in MeOH:$H_2O$ (9:1, v:v) without irradiation.

## 2.13. Calculation of quantum yields

Based on the time dependent absorbance *A* of the 452 nm band the decay rate of the concentration of $[Ru(bpy)_3]^{2+}$ was determined. Concentration was calculated using Beer-Lambert law: [4]

$$c(t) = \frac{A(t)}{\varepsilon \cdot d} \qquad (9)$$

Here $\varepsilon$ is the absorption coefficient of 14 600 L mol$^{-1}$ cm$^{-1}$,[5] $d$ is the thickness of the cuvette (1 cm). The values for the concentration can be found in the supporting data. The slope of the concentration against time was calculated and represents the changing rate $r$ of the $[Ru(bpy)_3]^{2+}$ concentration. Here we assume a pseudo-first order for the degradation of the **PS**.

$$r = \frac{\Delta c}{\Delta t} \tag{10}$$

With the incident photon fluence rate $q$ (equation 6), the transmission of the sample $T$ (0.26 for a path length of 20 mm in the cuvette (filling height) and therefore an absorbance of 0.58), the volume $V$ of the sample (2 mL) and the changing rate of the concentration $r$ the quantum yield is calculated using the following equation:

$$\Phi = \frac{r * V}{q * T} \tag{11}$$

# 3. Computational Data

The ORCA 6.1. [6] computational software was used to carry out optimization and TD-DFT UV-Vis calculations. This work used the Becke 3-Parameter Lee-Yang-Parr (B3LYP)[7] at the hybrid level of theory. This functional was chosen based on previous studies.[8] The def2-type basis set of triple-zeta quality within the valence region, with an additional polarization function (def2-TZVP)[9], was employed together with Grimme's D3BJ dispersion correction, as implemented in the ORCA 6.1. software package to account for any longer-range interactions.[10,11] The effective core potentials (ECPs) for molybdenum were likewise taken from the ORCA 6.1 implementation.[12] For the TD-DFT calculations specifically, 100 transitions are calculated per geometry.

## 3.1. Simulated UV/Vis spectra

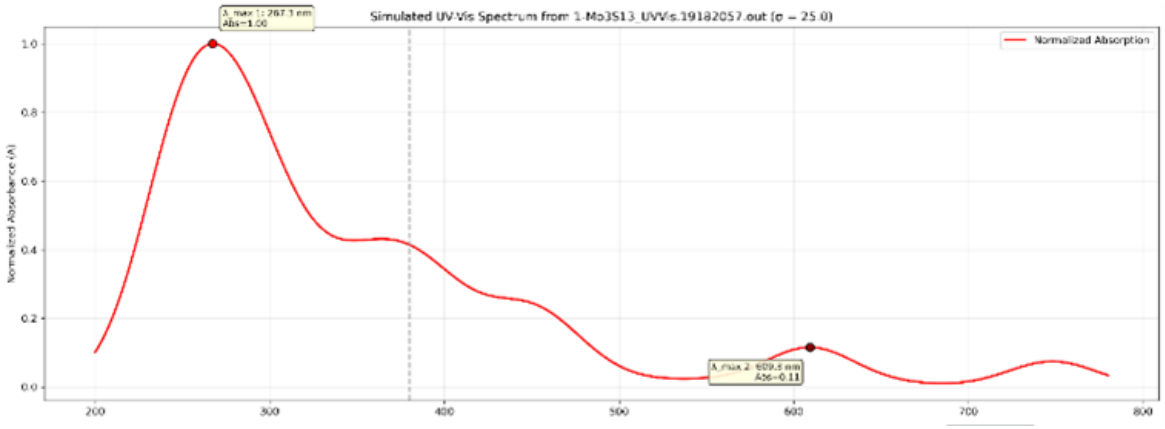


Figure S16: DFT-simulated UV/Vis spectrum of the **{Mo3}** cluster.

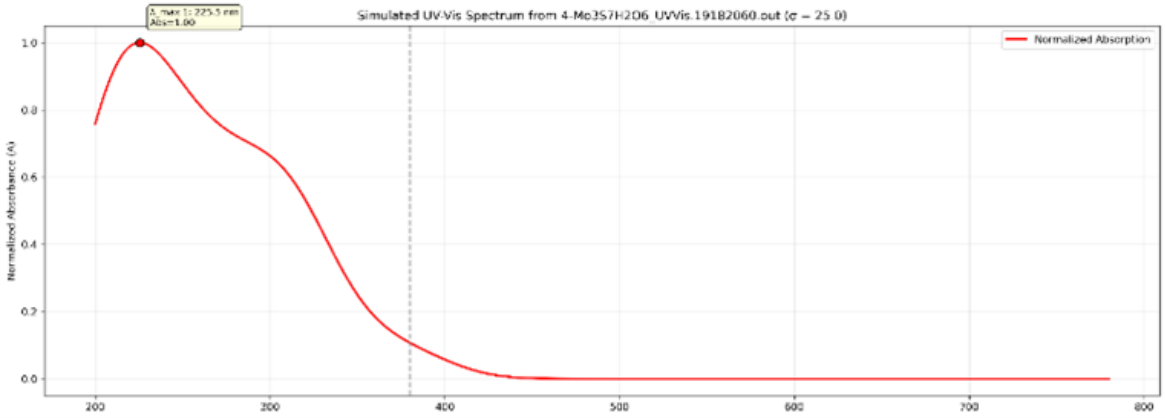

Figure S17: DFT-simulated UV/Vis spectrum of $[Mo_3S_7(H_2O)_6]^{4+}$.

Over the course of ligand exchange the change and reduction of transitions involving ligand centers is assumed. Those transition states may correlate to LMCT states or similar mixed states. The respective transition bands may be around 750 nm, 610 nm, 450 nm, 380 nm.
In the final species, $[Mo_3S_7(H_2O)_6]^{4+}$, a new mixed transition state around 300 nm was calculated, which involves the bridging disulfide ligands, which had not been involved for most of the significant LMCT states mentioned above.

## References


1 A. Müller, E. Diemann, R. Jostes and H. Bögge, *Angewandte Chemie International Edition in English*, 1981, 20, 934–955.

2 D. Kowalczyk, P. Li, A. Abbas, J. Eichhorn, P. Buday, M. Heiland, A. Pannwitz, F. H. Schacher, W. Weigand, C. Streb and D. Ziegenbalg, *ChemPhotoChem,* 2022, 6, DOI:10.1002/cptc.202200044.

3 E. F. Schuberiil, *Light Emitting Diodes*, 3rd Edition *E. Fred Schubert,* 2018.

4 A. Beer, *Annalen der Physik und Chemie*, 1852, 86, 78–88.

5 I. M. Dixon, S. Bonnet, F. Alary and J. Cuny, *Journal of Physical Chemistry Letters*, 2021, 12, 7278–7284.

6 F. Neese, *Wiley Interdisciplinary Reviews: Computational Molecular Science*, 2025, 15, e70019.

7 A. D. Becke, *The Journal of Chemical Physics*, 1993, 98, 5648–5652.

8 M. Dave, A. Rajagopal, M. Damm-Ruttensperger, B. Schwarz, F. Nägele, L. Daccache, D. Fantauzzi, T. Jacob and C. Streb, *Sustainable Energy Fuels*, 2018, 2, 1020–1026.

9 F. Weigend and R. Ahlrichs, *Physical Chemistry Chemical Physics*, 2005, 7, 3297–3305.

10 S. Grimme, S. Ehrlich and L. Goerigk, *Journal of Computational Chemistry*, 2011, 32, 1456–1465.

11 S. Grimme, J. Antony, S. Ehrlich and H. Krieg, *Journal of Chemical Physics*, 2010, 132, DOI:10.1063/1.3382344/926936.

12 D. Andrae, U. Häußermann, M. Dolg, H. Stoll and H. Preuß, *Theoretica Chimica Acta*, 1990, 77, 123–141.